

Centimeter-Sized Dried Foam Films of Graphene: Preparation, Mechanical and Electronic Properties

Wufeng Chen and Lifeng Yan*

A foam film is a typical 2D assembly of amphiphilics with a regular molecular arrangement, and such a structure is usually obtained by contacting air bubbles in surfactant solution or expanding the bubbles at the air/water interface.^[1] Thin dried foam films can be generated when interstitial water drains away in air, which can be used as a template to prepare self-standing ultrathin films of surfactants and inorganic sheets in micrometer sizes.^[2] Mechanistic studies reveal that dried films are formed by slowly evaporating the solution of amphiphilic compounds in the holes of substrates due to the spontaneous head-to-head arrangement of their hydrocarbon chains directed towards the air.^[2a] However, it is still difficult to prepare centimeter-sized thin films by this method and only small dried foam films or their arrays have been successfully prepared due to the weak stability of the head-to-head arrangement of surfactant molecules. We speculate that it might be possible to fabricate a centimeter-sized thin film if 2D nanosheets are used as the building blocks instead of traditional linear small surfactant molecules, and the overlap of 2D nanosheets should provide a new kind of arrangement, especially the layer-by-layer self-assembly in the direction parallel to the interface. Graphene, the single 2D sheet of carbon atoms patterned in the honeycomb lattice form, has recently attracted much attention for its unique electronic properties, excellent mechanical properties, and superior thermal properties.^[3] It has been reported that graphene oxide (GO) is a kind of colloidal surfactant due to its amphiphilic characteristics,^[4] and it can easily self-assemble into films via π - π stacking interactions.^[5] The nanometer pores in the graphene film are also advantageous to the design of materials for filtration and separation.^[6]

Graphene is a potential material to replace indium tin oxide (ITO) or fluorine tin oxide (FTO) due to its remarkable electronic properties. It has been reported that the transmittance of mechanically exfoliated graphene is 97.7% and for graphene synthesized by chemical vapor deposition (CVD) it is 97.4%.^[7] The sheet resistance (R_s) of graphene is another key parameter, which depends strongly on the film's surface morphology and the quality of the crystals. However, it is still a challenge to obtain graphene films with a low R_s value. CVD could produce highly conductive graphene films with R_s of about $275 \Omega \square^{-1}$

for a single layer and about $40 \Omega \square^{-1}$ for four layers doped with HNO_3 .^[8] Nevertheless, novel and simple methods still need to be developed for the preparation of graphene films with high electrical conductivity and transparency, especially at a large scale. Langmuir–Blodgett (LB),^[9] vacuum filtration,^[10] evaporation-induced self assembly,^[11] spray-coating,^[12] spin-coating,^[13] and bubble deposition^[5] methods have been employed to prepare graphene films. For example, spray-coated films of graphene show transparencies of about 90% and R_s about $5 \text{ k}\Omega \square^{-1}$,^[12] while 83% transparency and R_s of $8 \text{ k}\Omega \square^{-1}$ were obtained for graphene films prepared by the LB method.^[9] Graphene films prepared by spin-coating followed by a thermal graphitization procedure at 1100°C show a transparency of 80% and R_s of 10^2 – $10^3 \Omega \square^{-1}$.^[13] Thus, it is still necessary to develop novel methods to prepare centimeter-sized thin films of graphene with a high transparency and electrical conductivity.

Figure 1a,b show the processes employed for the fabrication of the target centimeter-sized thin films of graphene oxide via the dried foam film technique. The formation of traditional dried foam films of surfactants on a hole of substrate has been well studied, and a two-step mechanism is involved: first, a small volume of an aqueous solution of surfactant is captured in a hole by dipping, and then the surfactant molecules spontaneously self-assemble into two Gibbs monolayers at the air–water interface during the evaporation of water.^[2a] The two monolayers gradually get closer to each other and finally form a free-standing reversed bilayer, as shown in Figure 1a.^[2b] When we use GO to replace the traditional surfactants, the process should be different due to the fact that GO is a 2D nanosheet. The evaporation of water can also induce the self-assembly of GO nanosheets, but they will not arrange in a head-to-head manner, as is the case for surfactant molecules, and should be in the layer-by-layer form. The driving force is the π - π stacking and hydrogen bonding interactions among adjacent GO nanosheets. The driving force is so strong that it can support the formation of centimeter-sized thin films of GO with diameters of centimeters (Figure 1b). The as-prepared GO film is stable and has a high transparency. As shown in Figure 1c, GO thin films the size of micrometers can be easily prepared by dipping a copper microgrip into the aqueous dispersion of GO and subsequently drying it in air. The copper microgrid has a regular array of holes of $140 \mu\text{m} \times 140 \mu\text{m}$. The scanning electron microscopy (SEM) image in Figure 1c clearly shows a high coverage of the holes by the formed GO films, as well as a few broken films (Figure 1d). The wrinkle of the upside film reveals the shrink of the film after breaking, indicating the higher inner tensile force which can damage the film. Ultrathin dried foam films of GO can also be directly prepared by using a large size ring of Ag wire as a template, and a large circular GO film is formed under the assistance of a small amount of surfactant

Dr. W. F. Chen, Prof. L. F. Yan
Hefei National Laboratory for Physical Sciences at
the Microscale and Department of Chemical Physics
CAS Key Laboratory of Soft Matter Chemistry
University of Science and Technology of China
Hefei, 230026, PR China
E-mail: lfyan@ustc.edu.cn



DOI: 10.1002/adma.201203222

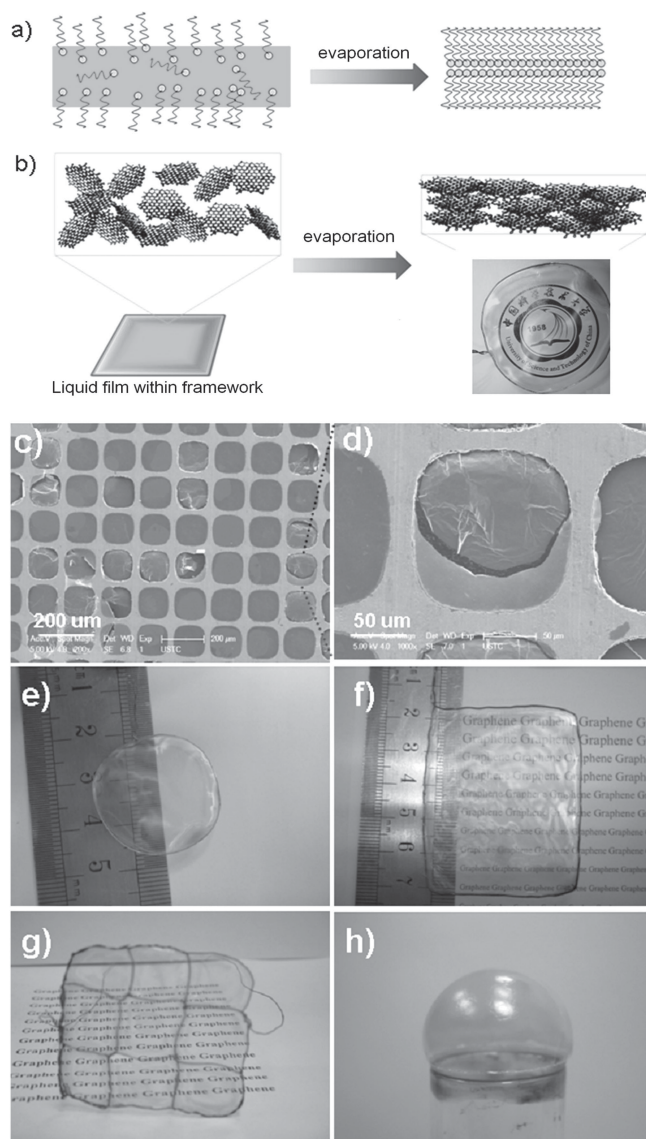


Figure 1. Schematic diagram showing the formation of a dried foam film of surfactant in a micrometer hole (a), and the formation of a dried foam film of GO (b). Dried foam films of GO prepared on different templates: SEM images of GO ultrathin films on a copper microgrid at different scales (c,d), with GO: 2.5 mg mL⁻¹; GO ultrathin film formed on an Ag circular template with diameter of centimeters (e), with GO: 4 mg mL⁻¹; GO ultrathin film formed on a Ag quadrangular template in size of centimeters (f), with GO: 12.0 mg mL⁻¹; GO ultrathin film formed on a huge Ag grid template (g), with GO: 6.0 mg mL⁻¹; GO ultrathin film formed on a hemispherical bubble template with a size of several centimeters (h), with GO: 8.0 mg mL⁻¹.

cetyltrimethylammonium bromide (CTAB) (Figure 1e). The diameter is about 2.7 cm, which is the biggest dried foam film ever reported. Importantly, the as-formed GO film is of high transparency, indicating the close packing of GO nanosheets. Figure 1f shows a larger transparent dried foam film of GO in a rectangle template, and the size is 5.4 × 4.1 cm². What would happen if a huge metal grip is used as a template? Figure 1g shows a large GO film formed on a huge grid of Ag wire with

3 × 3 rectangles. Interestingly, a huge consecutive GO film is obtained, and this method makes it possible to prepare very large GO films.

In addition, graphene on a metallic grid is also a useful route to preparing high-performance transparent electrodes, and the huge graphene ultrathin film on a Ag grid is attractive.^[14] A global photoelectronic device may be another intriguing method, and bubble templates can be used to prepare hemispherical dried foam films of GO. As shown in Figure 1h, a hemispherical GO film with high transparency has been successfully prepared at the end of a tube with a diameter of centimeters. Clearly, compared with the spin-coating and layer-by-layer assembly reported for the preparation of graphene films, the new method is simple and can be used to prepare free-standing graphene films of varying thicknesses and sizes, even in curved shapes.

The microstructures of the as-prepared thin dried foam films of GO have been studied by means of atomic force microscopy (AFM), SEM, and transmission electron microscopy (TEM). The size of GO nanosheets is in the range of nanometers to micrometers, with the typical thickness is 1.1 nm, indicating a single layer of GO (Figure 2a). However, after the formation of the dried foam film, the boundary of individual GO nanosheets disappears, indicating the overlap of the nanosheets during the formation of the film. The section line analysis gives the thickness of the GO film as 14.7 nm (Figure 2b), indicating the formation of ultrathin GO films. The result is also supported by the SEM measurement (Figure 2c.) The surface of as-prepared GO ultrathin films is smooth at the macroscopic scale. However, AFM (Figure 2d) and SEM (Figure 2e) studies clearly show that there are some quasi-one-dimensional creases with a length scale of 0.3–10 μm and a height of 2–10 nm, which were formed by the overlap of GO sheets where some of the GO edges were scrolled or folded during film fabrication.^[15] A TEM image and the related SAED pattern are shown in Figure 2f, also revealing that an as-formed GO ultrathin film results from the overlap of GO nanosheets. The formed liquid crystal phase of GO nanosheets in the aqueous suspension and liquid film is the key step for the self-assembly (Supporting Information, Figure S3), and a possible mechanism may include several steps, such as the change from an isotropic GO dispersion to a nematic liquid crystalline GO, and then to a lamellar GO film.^[16]

Thermal reduction (or a combination with chemical pre-reduction with N₂H₄) is the most efficient method to achieve highly conductive reduced GO (rGO) films.^[17] The as-prepared GO ultrathin film can be transferred from a circular template onto the surface of a glass substrate, and then it was reduced by heating the sample at 800 °C for 3 h under vacuum (Figure 3a). After thermal reduction, the film becomes a little black, and the transmittances of the as-formed rGO ultrathin film depend on the thickness of GO ultrathin film, with the thinner GO film having a higher transparency (Figure 3a,b). Figure 3e shows the transparency of the GO and rGO films (Figure 3b), and the as-formed GO film shows a very high transparency of 95.3% at 550 nm and 98.8% at 1000 nm, indicating good stacking of the GO nanosheets. However, after chemical reduction by HI, the transparency decreases and the transmittance is 71.2% at 550 nm and 75.8% at 1000 nm, while it is 63.1% at 550 nm for the rGO film prepared by combined chemical and thermal

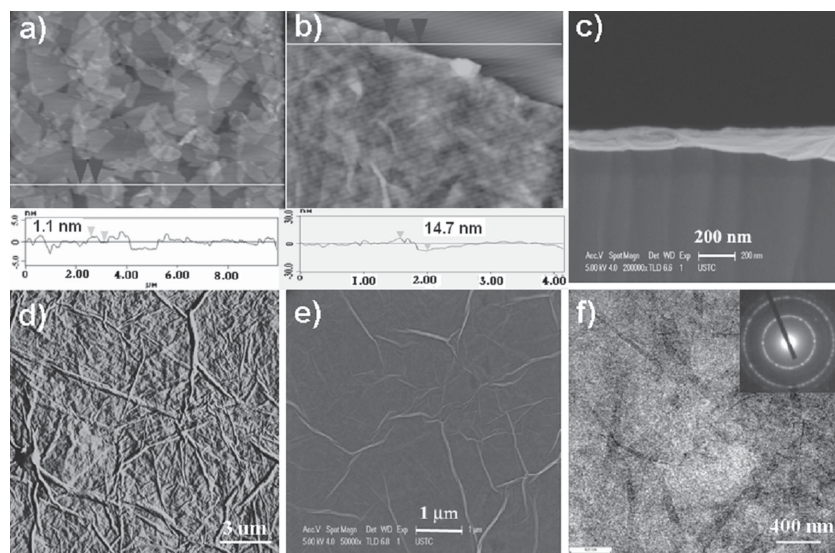


Figure 2. Microstructure of the as-formed centimeter-sized thin dried foam films of GO. (a) AFM height image and its section line analysis of the GO nanosheets. GO: 0.1 mg mL⁻¹. (b) AFM height image of an as-formed dried foam film of GO at the edge, and its section line analysis. (c) Cross-sectional SEM image of the as-prepared, ultrathin, dried foam film of GO. (d) AFM image of the ultrathin dried foam film of GO. (e) SEM image of the centimeter-sized thin dried foam film of GO. (f) TEM image of the centimeter-sized thin dried foam film of GO. Inset: The corresponding electron diffraction pattern. (b–f) GO: 2.5 mg mL⁻¹.

reduction. In addition, in contrast to ITO and FTO which show strong absorptions in the infrared region, the rGO ultrathin film remains transparent in this region. This unique optical property should render rGO ultrathin films appropriate for

broad application in optoelectronics. Interestingly, the as-formed GO ultrathin films can also be transferred to different kinds of substrates, such as flexible polymers. A circular dried GO ultrathin film was transferred onto a polyethylene terephthalate (PET) surface, and then it was reduced by concentrated HI ethanol solution. Figure 3c shows the macroscopic image of the sample, which maintains its high transparency even after bending several times, making it a potential material for flexible electronics. The electrical conductivities of the as-prepared rGO ultrathin films were measured by a two-point-probe method and the R_s is 920 $\Omega \square^{-1}$ for the rGO film shown in Figure 3a. The R_s value is similar to that of the graphene film prepared by spin-coating and vacuum annealing, and might be used as anodes to replace ITO in devices.^[18] For the flexible rGO ultrathin film on PET, the electrical conductivity is 3.61 k $\Omega \square^{-1}$. The higher resistance is caused by the chemical reduction, which is not as efficient as thermal reduction, however, its electrical conductivity still remains at 3.88 k $\Omega \square^{-1}$ after repeated bending 100 times, indicating that the bending process exhibits less effect on

its microstructure. Figure 3d shows the TEM image of the rGO ultrathin film as shown in Figure 3b: the surface of rGO film is flat and the relative SAED pattern studies reveal that the rGO ultrathin film is the overlap of rGO nanosheets. Figure 3f shows

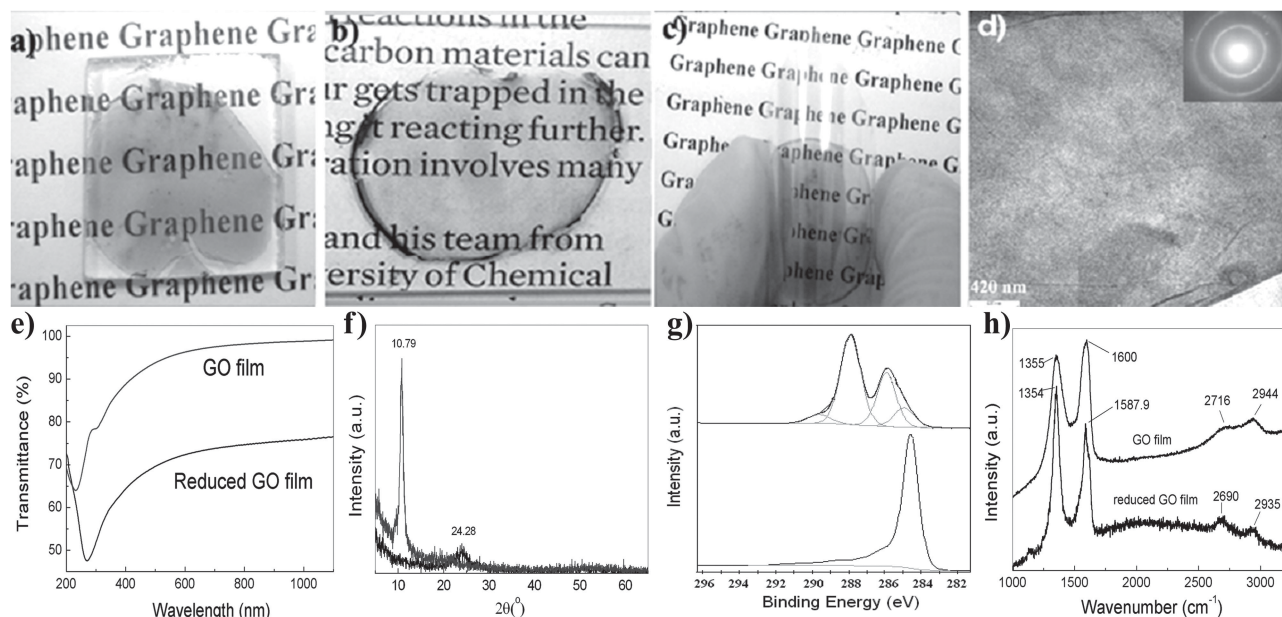


Figure 3. Reduced GO ultrathin films and their properties. (a) Photograph of an rGO film prepared by a thermal reduction of a chemically pre-reduced GO ultrathin film at 800 °C. (b) Photograph of an rGO ultrathin film prepared by chemical reduction of a GO film with a thickness of 14.7 nm. (c) rGO ultrathin film prepared by transferring the GO ultrathin films onto a flexible PET surface following a chemical reduction. (d) TEM image of the rGO film as shown in (a); inset shows the corresponding electron diffraction pattern. (e–h) Transmittances, XRD patterns, Raman spectra, and XPS profiles of the as-formed GO and rGO ultrathin films as shown in (b). GO: 2.5 mg mL⁻¹.

the X-ray diffraction (XRD) patterns of as-formed GO ultrathin film and the rGO ultrathin film after thermal reduction. For the GO ultrathin film there appears to be a wide diffraction peak at 10.4° , corresponding to a d -spacing of 0.83 nm. After thermal reduction, the peak at 10.4° disappears and there appears a new wide diffraction peak at 24.3° , corresponding to an interlayer spacing of 0.38 nm, which is still higher than that of pristine graphite (0.34 nm). This result reveals that the packing of rGO nanosheets becomes closer than that in the GO ultrathin film. Figure 3g shows the Raman spectra of GO and the thermally reduced GO ultrathin films. Both spectra show the existence of the D band and G band. For GO ultrathin films, the G band is located at 1600 cm^{-1} , while for the rGO ultrathin films the G band shifted to 1588 cm^{-1} , indicating the reduction of GO. At the same time the existence of a D band at 1355 and 1354 cm^{-1} for both GO and rGO ultrathin films indicates a defect in the sample. The intensity ratio of the D and G bands (I_D/I_G) changes from 0.95 to 1.17, indicating an increase in the average size of the sp^2 domain upon the reduction of GO. Figure 3h shows the XPS patterns of GO and rGO ultrathin films, respectively. For the GO ultrathin film, the C1s peak consists of three main components arising from C–O (hydroxyl and epoxy, 286.7 eV), C=O (carbonyl, 287.4 eV), and C=C/C–C (284.7 eV) species, and a weaker O=C–O (carboxyl, 288.8 eV) band. After chemical reduction, the oxygen-containing groups such as C–O (hydroxyl and epoxy, 286.5 eV), C=O (carbonyl, 287.9 eV), and O=C–O (carboxyl, 289.1 eV) reduced significantly, indicating an efficient reduction.

It is also possible to prepare thick dried foam films of GO by increasing the concentration of the GO aqueous solution. Figure 4a shows a cross-sectional SEM image of a GO film with a thickness of about 400 nm. The obtained GO film strips were employed for mechanical measurements. Figure 4b shows the stress–strain curve for the GO film. The deformation process of the film contains two steps: a self-reinforcement step (below 0.3% strain) and an elastic deformation step (up 0.3% strain). In the first step, the modulus increases quickly with the stress, indicating the self-orientation of tile-like lamellae structures under tensile loading.^[11,19] In the second step, a linear relationship between stress and strain appears, and the elastic modulus and tensile strength are evaluated to be 13.9 GPa and 62.7 MPa, respectively. These results reveal that the as-prepared dried foam film of GO is of high strength.

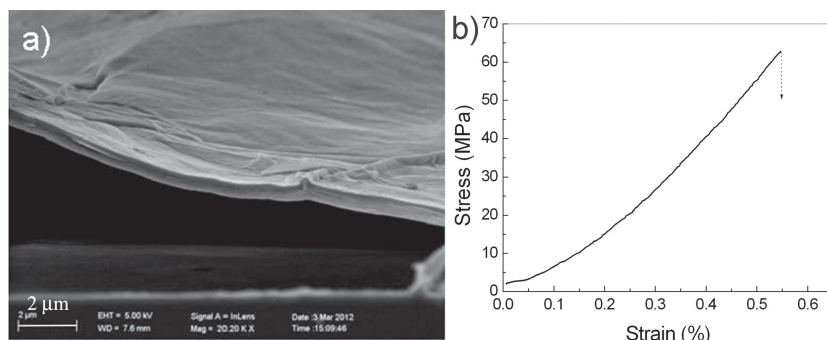


Figure 4. Mechanical properties of the dried foam film of GO. (a) Cross-sectional SEM image of the GO film in thickness of $\sim 400\text{ nm}$. (b) Stress–strain curve of the GO film. GO: 20.0 mg mL^{-1} .

In conclusion, we have developed a novel method for the fabrication of centimeter-sized free-standing ultrathin films of GO via the preparation of dried foam films. After chemical and/or thermal reduction, free-standing rGO films with a high electrical conductivity and transparency were prepared, which have potential application as electrode materials to replace ITO or FTO in flexible photoelectric devices. This method also has potential for the fabrication of 2D free-standing ultrathin films using graphene-like materials.

Experimental Section

Materials: Graphite powder, natural briquetting grade, ~ 100 mesh, 99.9995% (metals basis) was purchased from Alfa Aesar. Analytical grade NaNO_3 , KMnO_4 , 98% H_2SO_4 , 30% H_2O_2 aqueous solution, HI aqueous solution, butylamine, benzyl alcohol, cetyltrimethylammonium bromide (CTAB), and sodium dodecyl benzene sulfonate (SDBS) were purchased from Shanghai Chemical Reagents Company, and were used directly without further purification. Ultra-pure water ($18\text{ M}\Omega$) was produced by a Millipore System (Millipore Q, USA).

Preparation of GO: GO is prepared from natural graphite by a modified Hummers and Offema method.^[20] In brief, natural graphite powder (2 g) was added into a beaker (250 mL) and NaNO_3 (1 g) and H_2SO_4 (46 mL) were added subsequently under stirring in an ice-bath. Then KMnO_4 (6 g) was added slowly into the beaker under stirring condition and the temperature of the system was controlled up to 20°C . 5 min later the ice-bath was removed and the system was heated at 35°C for 30 min. Next water (92 mL) was slowly added into the system and it was stirred for another 15 min. Then hot water (80 mL) with 60°C and 3% H_2O_2 aqueous solution were added to reduce the residual KMnO_4 until the bubbling is disappeared. Finally, the system was centrifuged at 7200 rpm for 30 min, and the residue was washed by warm water until pH 3–4 of the upper layer of the suspension. The obtained sediment was re-dispersed into water and was treated by mild ultrasound for 15 min. A homogeneous suspension was collected after removing the trace black residues by centrifugation at 3000 rpm for 3 min. GO powder was obtained after freezing and drying of the suspension.

Preparation of Dried Foam Films of GO: First, aqueous solutions of GO in different concentrations ($2.0\text{--}20.0\text{ mg mL}^{-1}$) were prepared by dispersing GO in deionized water under mild ultrasound for 15 min, and then a small quantity of surfactant, such as CTAB or SDBS (0.02 mg mL^{-1}) was added. In some cases, butylamine (0.1 v%) and/or benzyl alcohol (0.5 v%) were added to replace CTAB or SDBS. Then a ring of Ag wire, tube, or porous substrates were vertically or horizontally dipped into the solution and gently lifted from the solution. A small volume of aqueous solution of GO was captured by the templates during the process, and the templates were then allowed to dry in air. Generally, the drying process was carried out at room temperature under the normal humidity condition ($\sim 20\%$). For a rapid GO foam film fabrication, it can also be dried in warm air of about 60°C . Dried foam films of GO in different scales, thickness and shapes were prepared by GO sheets spontaneous self-assembly at the air–water interface during the evaporation of water.

Preparation of Reduced Graphene Oxide (rGO) Films: Chemical and/or thermal reduction of GO to rGO films have been carried out. For chemical reduction, the as-prepared free-standing dried films of GO were transferred to a substrate such as glass, quartz or silica, and then they were reduced by concentrated ethanol solution of HI (30 v%) for 6 h at room temperature following washed by ethanol. For thermal reduction, the HI reduced GO films on quartz or silica substrates were loaded inside a 5 cm internal diameter quartz tube. The tube was

introduced into tube oven (OTF-1200X) fitted with controlled vacuum and gas flows. At first, a 10^{-5} Torr vacuum was created by a turbo pump with one open ends for 30 min, next the closed end was open and filled by a continuous flow of ultrapure argon (100 cm^3). The films were heated at a rate of $10\text{ }^{\circ}\text{C}/\text{min}$, held at $800\text{ }^{\circ}\text{C}$ for 3 h, and allowed to cool to room temperature over night.

Characterization: Wide-angle X-ray diffraction (XRD) analyses were carried out on an X-ray diffractometer (D/MAX-1200, Rigaku Denki Co. Ltd., Japan). The XRD patterns with Cu K α radiation ($\lambda = 1.5406$) at 40 kV and 100 mA were recorded in the range of $2\theta = 5\text{--}65^{\circ}$. A commercial atomic force microscope (AFM, Nanoscope IIIa; Digital Instruments, Santa Barbara, CA), equipped with a J scanner was used to measure the morphologies and thicknesses of the samples. Si_3N_4 tip (Nanoprobes, Digital Instruments Inc.) was used by the contact mode. The scan rates were between 1.0 and 2.4 Hz. Polarized optical microscopy (POM) observation were performed with a Nikon E600POL. X-ray photoelectron spectroscopy (XPS) were recorded on an Escalab MK II photoelectron spectrometer (VG Scientific Ltd., United Kingdom). Raman spectra were taken on a RAMAMLOG 6 (Spex, USA) using a $50\times$ objective lens with a 514.5 nm laser excitation. TEM images were measured on a Hitachi H-800 microscope at 200 kV. XPS spectra were recorded by an Escalab MK II photoelectron spectrometer (VG Scientific Ltd., United Kingdom). The structures of the films were measured using a Sirion 200 FESEM at an accelerating voltage of 10 kV. The mechanical performances of the GO films were measured by Dynamic Mechanical Analyzer DMA Q800, and the films were carefully cut into approximately $7\text{ mm} \times 35\text{ mm}$ strips before the tensile test, and the experiments were carried out under the conditions of 20% humidity at room temperature, and the initial tensile length of 20 mm and a drawing speed of $2\text{ mm}/\text{min}$. For the electrical conductivity measurement, the reduced GO film was patterned 100 nm gold contacts through a shadow mask, and then the sheet resistance was measured using a semiconductor parametric analyzer (Keithley 2420, Keithley Instruments Inc., Cleveland, OH).^[13] The drying process of the foam film was recorded by a metallurgical microscope (DMM-200C) using a $10\times$ objective lens without polarized light. Optical transmittance of the GO film was evaluated using a UV-vis-NIR spectrophotometer (Shimadzu UV-2401PC).

Supporting Information

Supporting Information is available from the Wiley Online Library or from the author.

Acknowledgements

This work is supported by the National Basic Research Program of China (No. 2011CB921403 and 2010CB923302), and the National Natural Science Foundation of China (No. 20874095 and No.51073147). Prof. Shiyong Liu and Quanxin Li are appreciated for their kindness help.

Received: August 5, 2012

Published online:

- [1] a) E. Sackmann, *Science* **1996**, 271, 43; b) J. Jin, W. Bu, I. Ichinose, *Langmuir* **2010**, 26, 10506.
- [2] a) J. Jin, J. Huang, I. Ichinose, *Angew. Chem. Int. Ed.* **2005**, 44, 4532; b) J. Jin, Y. Wakayama, X. Peng, I. Ichinose, *Nat. Mater.* **2007**, 6, 686.
- [3] a) A. K. Geim, K. S. Novoselov, *Nat. Mater.* **2007**, 6, 183; b) S. Stankovich, D. A. Dikin, G. H. B. Dommett, K. M. Kohlhaas, E. J. Zimney, E. A. Stach, R. D. Piner, S. T. Nguyen, R. S. Ruoff, *Nature* **2006**, 442, 282; c) F. Schedin, A. K. Geim, S. V. Morozov, E. W. Hill, P. Blake, M. I. Katsnelson, K. S. Novoselov, *Nat. Mater.* **2007**, 6, 652.
- [4] J. Kim, L. J. Cote, F. Kim, W. Yuan, K. R. Shull, J. X. Huang, *J. Am. Chem. Soc.* **2010**, 132, 8180.
- [5] J. L. Azevedo, C. Costa-Coquelard, P. Jegou, T. Yu, J.-J. Benattar, *J. Phys. Chem. C* **2011**, 115, 14678.
- [6] R. R. Nair, H. A. Wu, P. N. Jayaram, I. V. Grigorieva, A. K. Geim, *Science* **2012**, 335, 442.
- [7] a) K. S. Kim, Y. Zhao, H. Jang, S. Y. Lee, J. M. Kim, J. H. Ahn, P. Kim, J. Y. Choi, B. H. Hong, *Nature* **2009**, 457, 706; b) X. S. Li, W. W. Cai, J. H. An, S. Kim, J. Nah, D. X. Yang, R. Piner, A. Velamakanni, I. Jung, E. Tutuc, S. K. Banerjee, L. Colombo, R. S. Ruoff, *Science* **2009**, 324, 1312.
- [8] S. Bae, H. Kim, Y. Lee, X. F. Xu, J. S. Park, Y. Zheng, J. Balakrishnan, T. Lei, H. R. Kim, Y. I. Song, Y. J. Kim, K. S. Kim, B. Ozyilmaz, J. H. Ahn, B. H. Hong, S. Iijima, *Nat. Nanotechnol.* **2010**, 5, 574.
- [9] X. Li, G. Zhang, X. Bai, X. Sun, X. Wang, E. Wang, H. Dai, *Nat. Nanotechnol.* **2008**, 3, 538.
- [10] S. De, P. J. King, M. Lotya, A. O'Neill, E. M. Doherty, Y. Hernandez, G. S. Duesberg, J. N. Coleman, *Small* **2010**, 6, 458.
- [11] C. Chen, Q.-H. Yang, Y. Yang, W. Lv, Y. Wen, P.-X. Hou, M. Wang, H.-M. Cheng, *Adv. Mater.* **2009**, 21, 3007.
- [12] P. Blake, P. D. Brimicombe, R. R. Nair, T. J. Booth, D. Jiang, F. Schedin, L. A. Ponomarenko, S. V. Morozov, H. F. Gleeson, E. W. Hill, A. K. Geim, K. S. Novoselov, *Nano Lett.* **2008**, 8, 1704.
- [13] H. A. Becerril, J. Mao, Z. Liu, R. M. Stoltenberg, Z. Bao, Y. Chen, *ACS Nano* **2008**, 2, 463.
- [14] Y. Zhu, Z. Sun, Z. Yan, Z. Jin, J. M. Tour, *ACS Nano* **2011**, 5, 6472.
- [15] a) X. Wang, L. Zhi, K. Mullen, *Nano Lett.* **2007**, 8, 323; b) J. C. Meyer, A. K. Geim, M. I. Katsnelson, K. S. Novoselov, T. J. Booth, S. Roth, *Nature* **2007**, 446, 60.
- [16] Z. Xu, C. Gao, *ACS Nano* **2011**, 5, 2908.
- [17] S. Pang, Y. Hernandez, X. Feng, K. Müllen, *Adv. Mater.* **2011**, 23, 2779.
- [18] J. B. Wu, M. Agrawal, H. A. Becerril, Z. N. Bao, Z. F. Liu, Y. S. Chen, P. Peumans, *ACS Nano* **2010**, 4, 43.
- [19] D. A. Dikin, S. Stankovich, E. J. Zimney, R. D. Piner, G. H. B. Dommett, G. Evmenenko, S. T. Nguyen, R. S. Ruoff, *Nature* **2007**, 448, 457.
- [20] W. Chen, L. Yan, P. R. Bangal, *Carbon* **2010**, 48, 1146.